2552 J. Med. Chem. 2010, 53, 2552–2561
DOI: 10.1021/jm901773d

Journal of Medicinal Chemistry Article

Development of Novel Adenosine Monophosphate-Activated Protein Kinase Activators

Jih-Hwa Guh,[†,‡] Wei-Ling Chang,[†] Jian Yang,[†] Su-Lin Lee,[†] Shuo Wei,[†] Dasheng Wang,[†] Samuel K. Kulp,[†] and Ching-Shih Chen*[,†]

[†]*Division of Medicinal Chemistry, College of Pharmacy, The Ohio State University, 336 Parks Hall, 500 West 12th Avenue, Columbus, Ohio 43210, and* [‡]*School of Pharmacy, College of Medicine, National Taiwan University, Taipei, Taiwan*

Received November 30, 2009

In light of the unique ability of thiazolidinediones to mediate peroxisome proliferator-activated receptor (PPAR)γ-independent activation of adenosine monophosphate-activated protein kinase (AMPK) and suppression of interleukin (IL)-6 production, we conducted a screening of an in-house, thiazolidinedione-based focused compound library to identify novel agents with these dual pharmacological activities. Cell-based assays pertinent to the activation status of AMPK and mammalian homologue of target of rapamycin (i.e., phosphorylation of AMPK and p70 ribosomal protein S6 kinase, respectively) and IL-6/IL-6 receptor signaling (i.e., IL-6 production and signal transducer and activator of transcription 3 phosphorylation, respectively) in lipopolysaccharide (LPS)-stimulated THP-1 human macrophages were used to screen this compound library, which led to the identification of compound **53** (*N*-{4-[3-(1-methyl-cyclohexylmethyl)-2,4-dioxo-thiazolidin-5-ylidene-methyl]-phenyl}-4-nitro-3-trifluoro-methyl-benzenesulfonamide) as the lead agent. Evidence indicates that this drug-induced suppression of LPS-stimulated IL-6 production was attributable to AMPK activation. Furthermore, compound **53**-mediated AMPK activation was demonstrated in C-26 colon adenocarcinoma cells, indicating that it is not a cell line-specific event.

Introduction

The functional role of adenosine monophosphate-activated protein kinase (AMPK[a]) in regulating energy homeostasis and insulin sensitivity at both cellular and whole body levels has been well recognized.[1−3] In response to stimuli such as exercise, cellular stress, and adipokines, this cellular fuel-sensing enzyme induces a series of metabolic changes to balance energy consumption, including stimulation of glucose and fatty acid uptake, fatty acid oxidation, and mitochondrial biogenesis, and inhibition of glycogen synthesis, via multiple downstream signaling pathways controlling nutrient uptake and energy metabolism. More recently, accumulating evidence suggests a link between AMPK and cancer cell growth and survival in light of its ability to activate tuberous sclerosis complex 2, a tumor suppressor that negatively regulates protein synthesis by inhibiting mammalian homologue of target of rapamycin (mTOR).[4] From a mechanistic perspective, AMPK integrates growth factor signaling with cellular metabolism through the negative regulation of mTOR. In addition, AMPK has been reported to suppress inflammatory responses by inhibiting the production of inflammatory cytokines, especially interleukin (IL)-6, in macrophages.[5,6] Together, these findings suggest that AMPK represents a therapeutically relevant target for the treatment of type II diabetes, the metabolic syndrome, and cancer.[7−10]

A number of antidiabetic agents, including the stable AMP analogue 5-aminoimidazole-4-carboxamide ribose (AICAR), the thiazolidinedione family of PPARγ agonists, and metformin, are accepted pharmacological activators of AMPK although via distinct mechanisms.[11−13] These AMPK activators mediate indirect AMPK activation by mimicking AMP or altering cellular energy status[9] but suffer from low potency and/or "off-target" effects. For example, AICAR, after being converted to its monophosphate, mimics AMP to activate AMPK and its upstream kinase LKB1.[14] However, it exhibits an IC_{50} (the half maximal inhibitory concentration) in the mM range and has the potential to activate other AMP-sensitive enzymes.[15] More recently, a number of novel direct AMPK activators have been discovered, some of which exhibited promising in vitro and/or in vivo activities via the stimulation of AMPK function.[16−19]

In light of the unique ability of the thiazolidinedione family of PPARγ agonists to mediate PPARγ-independent activation of AMPK, we hypothesized that these agents could be pharmacologically exploited to develop potent AMPK activators by dissociating these two pharmacological activities. In this study, we conducted a two-tiered screening of an in-house, thiazolidinedione-based focused compound library to identify novel agents that, at low μM concentrations, exhibited the ability to activate AMPK and to inhibit IL-6 production independently of PPARγ in human THP-1 macrophages.

*To whom correspondence should be addressed. Phone: (614)-688-4008. Fax: (614)-688-8556. E-mail: chen.844@osu.edu.

[a]Abbreviations: AICAR, 5-aminoimidazole-4-carboxamide ribose; AMPK, adenosine monophosphate-activated protein kinase; ELISA, enzyme-linked immunosorbent assay (ELISA); FBS, fetal bovine serum; IC_{50}, the half maximal inhibitory concentration; JNK, Jun N-terminal kinase (JNK); IL-6, interleukin-6; LPS, lipopolysaccharide; mTOR, mammalian homologue of target of rapamycin; MTT, 3-(4,5-dimethylthiazol-2-yl)-2,5-diphenyltetrazolium bromide); p70S6K, p70 ribosomal protein S6 kinase; PMA, phorbol 12-myristate 12-acetate; PPARγ, peroxisome proliferator-activated receptor γ; PPRE, PPAR response element; Stat3, signal transducer and activator of transcription 3.

 Published on Web 02/19/2010

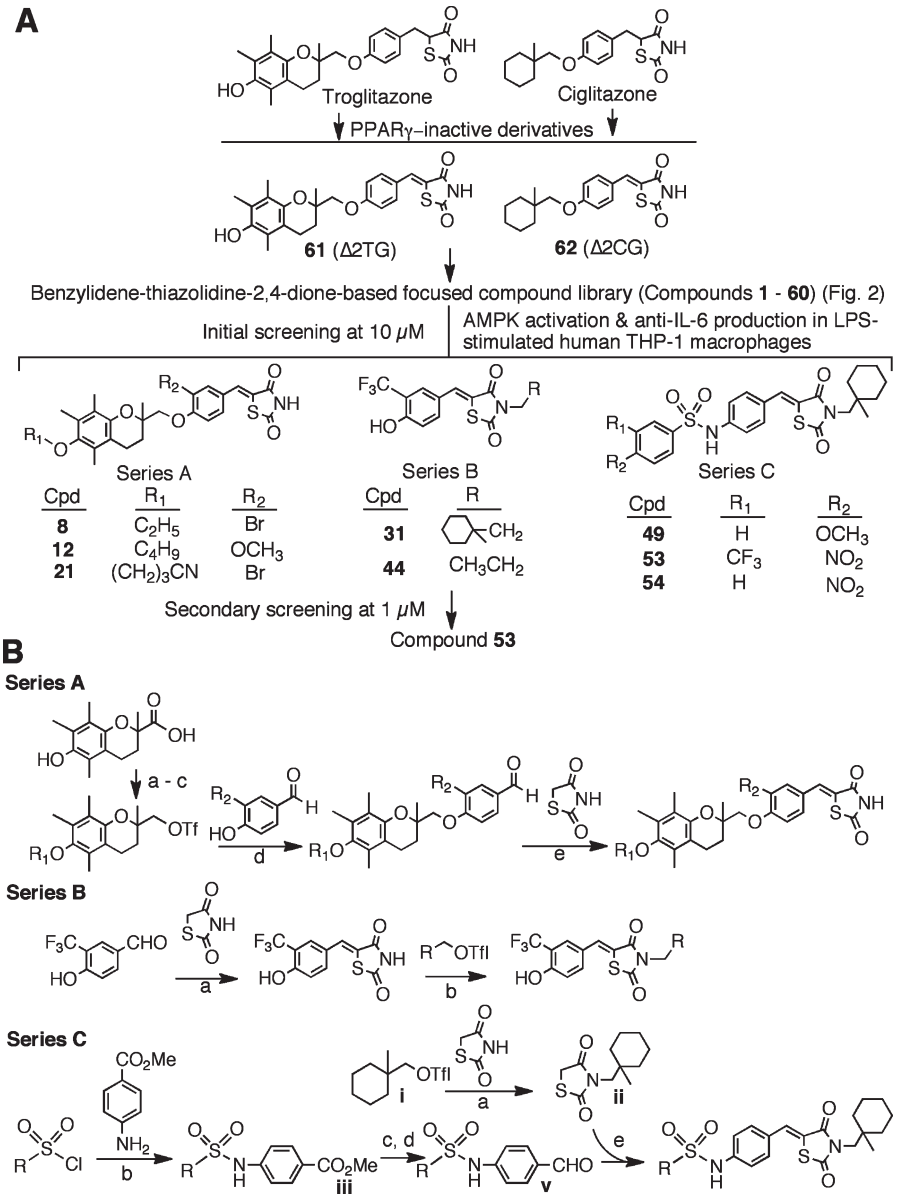

Figure 1. (A) Schematic representation of the two-tiered screening of the benzylidene-thiazolidinedione-based focused compound library to identify lead AMPK activators. (B) General synthetic procedure for series A−C compounds. Reaction conditions: Series A: a, K_2CO_3/R1-Br; b, LAH, THF; c, $(CF_3SO_2)_2O$, pyridine, CH_2Cl_2; d, K_2CO_3, DMF; e, AcOH, piperidine, ethanol/reflux. Series B: a, AcOH, piperidine, ethanol/reflux; b, K_2CO_3, DMF. Series C: a, K_2CO_3, DMF; b, pyridine, CH_2Cl_2; c, LAH, dry THF, 0 °C; d, MnO_2, CH_2Cl_2, reflux; d, piperidine, EtOH, reflux; e, AcOH, piperidine, ethanol/reflux.

Chemistry

Previously, we reported that introduction of a double bond adjoining the thiazolidinedione ring abrogated the PPARγ ligand property of troglitazone and ciglitazone (Figure 1A).[15] To abolish the PPARγ activity, we used the unsaturated derivatives of troglitazone and ciglitazone **61** (Δ2TG)[20] and **62** (Δ2CG)[21] as scaffolds to develop a focused compound library consisting of 60 compounds (**1**−**60**; Figure 2). Cell-based assays pertinent to the activation status of AMPK and mTOR [i.e., phosphorylation of AMPK and p70 ribosomal protein S6 kinase (p70S6K), respectively] and IL-6/IL-6 receptor signaling [i.e., IL-6 production and signal transducer and activator of transcription 3 (Stat3) phosphorylation, respectively] in lipopolysaccharide (LPS)-stimulated THP-1 macrophages were used to screen this compound library via Western blotting and enzyme-linked immunosorbent assay (ELISA) (Figure 3A). The first-tier screening of individual compounds at 10 μM netted eight active agents (**8**, **12**, **21**, **31**, **42**, **49**, **53**, and **54**), which were classified into three structural series (Figure 1A). A further examination of the ability of these agents at 1 μM to block the LPS-stimulated production of IL-6 identified compound **53** as the optimal agent. General procedures for the synthesis of series A−C compounds are depicted in Figure 1B.

Results

Proof-of-Concept That Thiazolidinediones Can Be Structurally Optimized to Develop Potent AMPK Activators. In this study, we used phorbol 12-myristate 12-acetate (PMA)-differentiated THP-1 cells, a cell line model mimicking many characteristic features of primary macrophages,[22] to examine the effect of thiazolidinedione derivatives on AMPK

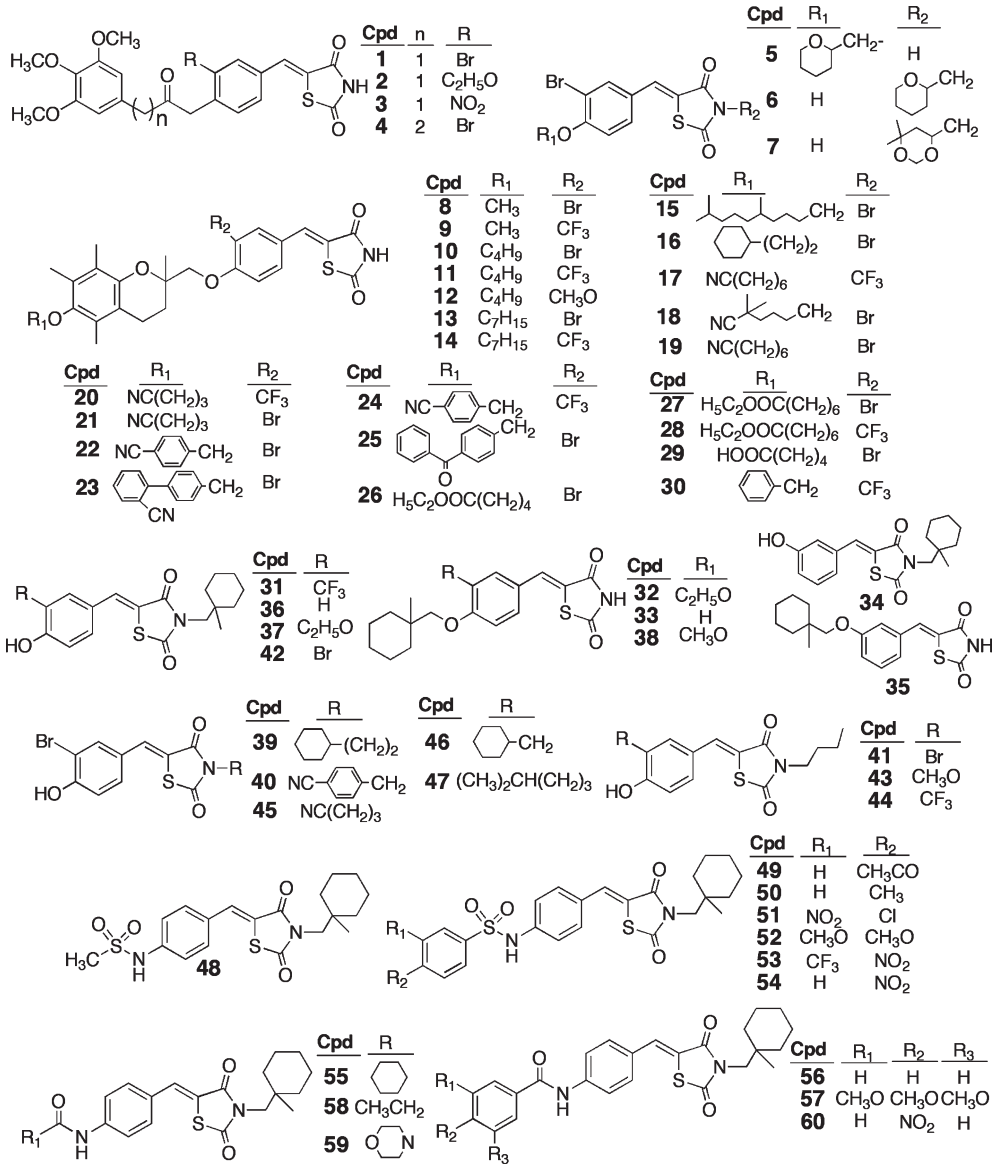

Figure 2. Chemical structures of compounds **1**−**60** in the thiazolidinedione-based focused compound library.

activation and LPS-induced mTOR activation and IL-6 secretion into the medium. In addition, the phosphorylation of p70S6K and Stat3 were monitored as markers for the activation status of mTOR and IL-6 receptor signaling pathways, respectively, in drug-treated cells (Figure 3A). Consistent with a recent report that high doses of ciglitazone ($\geq$100 μM) were required to activate AMPK,[23] our data indicate that ciglitazone at 10 μM exhibited no appreciable effect on the levels of p-AMPK or p-p70S6K relative to the LPS-treated control after 6 h of treatment (Figure 3B). In contrast, its PPARγ-inactive counterpart **62** at the same concentration was effective in elevating the level of p-AMPK, accompanied by a parallel decrease in p70S6K phosphorylation. Nevertheless, ciglitazone displayed a several-fold higher potency than **62** in inhibiting LPS-stimulated IL-6 production (Figure 3C), suggesting that the anti-IL6 activity of ciglitazone was primarily attributable to a PPARγ-dependent mechanism. This reduction in IL-6 production was not due to drug-induced cell death as neither agent inhibited the viability of THP-1 cells within the dose range examined. Moreover, the ability of ciglitazone and **62**, at 10 μM, to suppress LPS-activated IL-6 receptor signaling was evident by reduced Stat3 phosphorylation relative to the control (Figure 2B).

Screening of an In-House, Benzylidene-Thiazolidinedione-Based Focused Compound Library to Identify Effective AMPK Activators with High Potency in Suppressing IL-6 Production. On the basis of the above finding, we used **61** and **62** as scaffolds to generate a focused compound library consisting of 60 derivatives with diverse structures in which **62** was blindly embedded as a control (compound **33**) during the screening process (Figure 2). These compounds along with ciglitazone, each at 10 μM, were assessed for their abilities to activate AMPK and to inhibit IL-6 production in LPS-stimulated THP-1 cells (Figure 4). Consistent with the earlier finding, 10 μM **62** exhibited modest activities in AMPK activation and against IL-6 secretion, in conjunction with the inhibition of the phosphorylation of p70S6K and Stat3, while 10 μM ciglitazone was effective in inhibiting IL-6 production without affecting AMPK phosphorylation status. Of the other compounds examined, eight derivatives (**8**, **12**, **21**, **31**, **44**, **49**, **53**, **54**) exhibited substantially higher

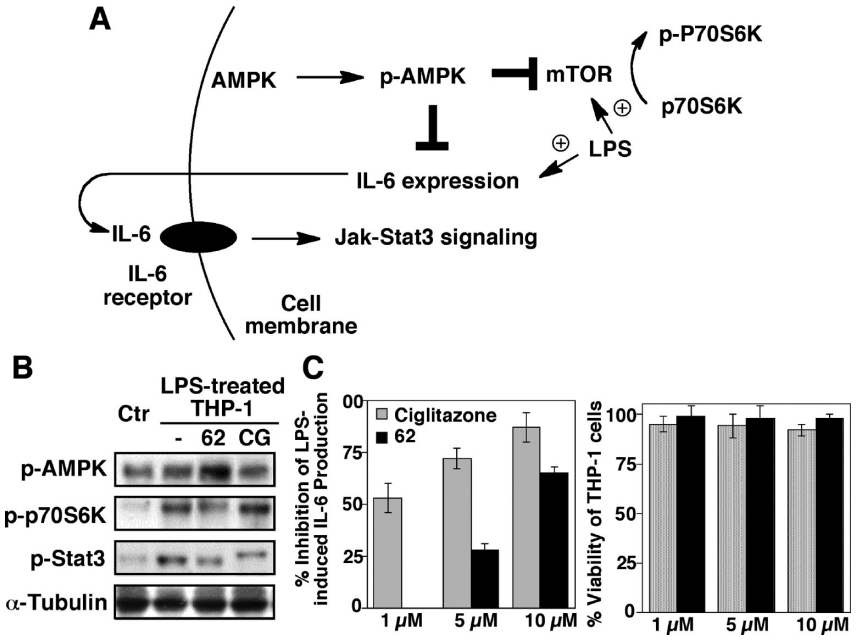

Figure 3. (A) Schematic representation of the role of AMPK as a negative regulator of mTOR- and IL-6/IL-6 receptor-mediated signaling pathways. (B) Western blot analysis of the effects of ciglitazone and **62**, each at 10 μM, on the phosphorylation of AMPK, p70S6K, and Stat3 in LPS-treated THP-1 cells relative to that on LPS-treated and untreated (Ctr) THP-1 macrophages in 10% FBS-containing medium after 6 h of treatment. (C) Left panel, ELISA analysis of the inhibitory effects of ciglitazone (CG) and **62** at the indicated concentrations on LPS-stimulated IL-6 production in THP-1 macrophages in 10% FBS-containing medium after 6 h of treatment. Columns, mean; bars, SD ($N = 3$). Right panel, the corresponding effects on the viability of THP-1 cells by MTT assays ($N = 6$).

potencies relative to **62** in the overall assessment of all of these markers (Figure 4; only those with greater than 80% inhibition of IL-6 production were selected). Again, none of these agents caused significant suppression of THP-1 cell viability (Figure 4B, lower panel), indicating that the inhibition of IL-6 production was not due to cell death. It is interesting to note that some of the agents in the library showed activities in AMPK activation but lacked effects on suppressing IL-6 production (e.g., compounds **4** and **5**) or vice versa (e.g., compounds **9**, **19**, **51**, **52**, **55**, and **59**), suggesting the involvement of alternative mechanisms in their modes of action.

To demonstrate that the drug-induced inhibition of IL-6 production was independent of PPARγ, we examined the ability of these eight agents versus ciglitazone to transactivate PPARγ by using the PPAR response element (PPRE) luciferase reporter assay. In THP-1 cells transiently transfected with a reporter construct (PPRE-x3-TK-Luc), ciglitazone at 10 μM significantly increased luciferase activity ($P < 0.001$) (Figure 5A). In contrast, none of the eight agents examined showed appreciable activity in PPARγ activation.

Compound 53 Represents the Lead Agent in AMPK Activation and IL-6 Repression. The activities of these candidate agents vis-à-vis ciglitazone in blocking IL-6 release were further assessed at 1 μM. As shown, compound **53** showed the highest potency, exceeding that of ciglitazone, followed by **54** and **49** (Figure 5B, upper panel), all three of which possess largely shared structural motifs with variations in substituents. Again, this inhibition of IL-6 production was not due to cell death as none of these agents exhibited a significant effect on THP-1 cell viability (lower panel).

Compound **53** inhibited LPS-stimulated IL-6 production in a dose-dependent manner, with an IC_{50} of approximately 1 μM (Figure 6A), paralleling its effect on the intracellular IL-6 mRNA expression (Figure 6B) and the phosphorylation levels of AMPK and p70S6K (Figure 6C). Moreover, the potency of compound **53** in activating AMPK is about two orders-of-magnitude higher than that of AICAR (Figure 6C).

To establish the mechanistic link between AMPK activation and anti-IL-6 activity, we examined the effect of the dominant-negative (DN) inhibition of AMPK via the ectopic expression of the K45R kinase-dead mutant (Figure 7A). Relative to the pCMV control, transient transfection of differentiated THP-1 cells with the DN-AMPK mutant significantly enhanced LPS-induced IL-6 production and reversed the inhibitory effect of compound **53** (10 μM) (Figure 7B). This finding suggests that AMPK activation is essential to the ability of compound **53** to suppress LPS-stimulated IL-6 production.

We further assessed the effect of compound **53** on the phosphorylation of AMPK and p70S6K in C-26 colon adenocarcinoma cells, a cell model commonly used for studying cancer cachexia.[24] Similar to that observed in THP-1 cells, compound **53** mediated robust increases in the p-AMPK level in dose- and time-dependent manners, accompanied by parallel decreases in p-p70S6K (Figure, 7C). It is noteworthy that this AMPK activation occurred almost immediately following drug treatment. Together, these findings confirmed that this drug effect was not a cell line-specific event.

Discussion

Recent evidence suggests that AMPK serves as a metabolic checkpoint by integrating growth factor signaling with cellular metabolism through the negative regulation of mTOR.[7−10] This unique functional role underscores the therapeutic value of targeting AMPK activation in different diseases ranging from insulin resistance to cancer through the regulation of energy metabolism. For example, a recent study demonstrates that AICAR was effective in suppressing the growth of EGFR-activated glioblastoma cells by inhibiting cholesterol and fatty acid biosynthesis.[25]

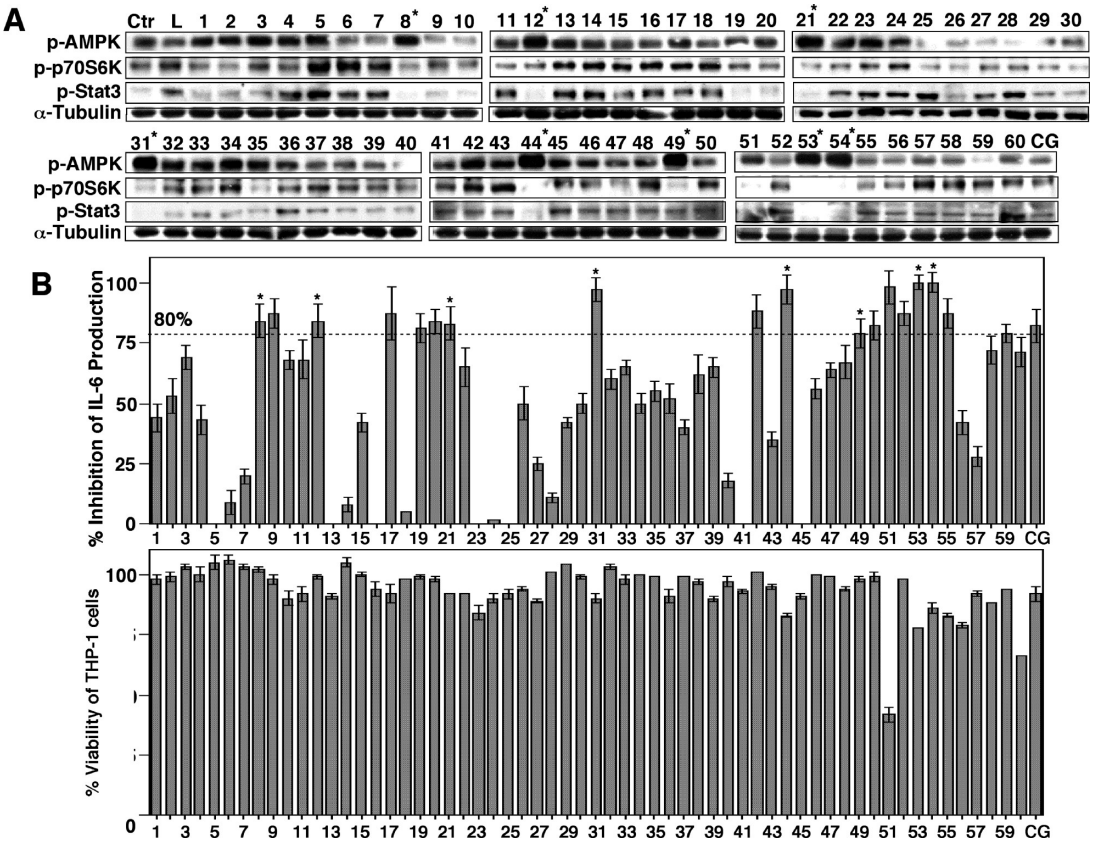

Figure 4. (A) Western blot analysis of the effects of compounds **1**−**60** vis-à-vis ciglitazone (CG), each at 10 μM, on the phosphorylation of AMPK, p70S6K, and Stat3 in LPS-treated THP-1 cells relative to that in LPS only treated (L) and untreated (Ctr) THP-1 macrophages in 10% FBS-containing medium after 6 h of treatment. (B) Upper panel, ELISA analysis of the inhibitory effects of compounds **1**−**60** vis-à-vis ciglitazone (CG), each at 10 μM, on LPS-stimulated IL-6 production in THP-1 macrophages in 10% FBS-containing medium after 6 h of treatment. Columns, mean; bars, SD ($N = 3$). Lower panel, the corresponding effects on the viability of THP-1 cells by MTT assays ($N = 6$).

Thus, this study was aimed at the pharmacological exploitation of thiazolidinediones to develop novel AMPK activators. Although AMPK is a highly conserved sensor of cellular energy status, its functional role varies in a cell context- and cell type-specific manner. Here, we used differentiated THP-1 macrophages as a cellular platform to conduct drug screening in light of the pivotal role of AMPK, as a negative regulator of mTOR, in promoting the anti-inflammatory phenotype of macrophages by suppressing the production of inflammatory cytokines such as IL-6.[6] By screening an in-house, thiazolidinedione-based focused compound library, this cell-based assay identified compound **53** as the lead agent with low μM potency in activating AMPK and inhibiting LPS-induced IL-6 secretion in THP-1 cells. We further demonstrated that this drug-induced suppression of LPS-stimulated IL-6 production was attributable to AMPK activation, which contrasts with the PPARγ-dependent mechanism of ciglitazone. Nevertheless, it was found that a number of the agents examined, although inactive in AMPK activation, exhibited significant effect on IL-6 production (compounds **9**, **19**, **51**, **52**, **55**, and **59**). From a mechanistic perspective, separation of these two pharmacological activities suggests diversity in the mode of action among these pharmacological agents, which warrants investigation. The premise is manifest by the ability of a number of small-molecule agents to modulate IL-6 production through distinct mechanisms. For example, luteolin, a flavonoid, reduced LPS-induced IL-6 production by inhibiting the Jun N-terminal kinase (JNK)-activator protein 1 pathway,[26] while chloroquine-mediated inhibition of IL-6 expression was associated with reduced mRNA stability and mRNA levels.[27] In addition, the bisphosphonate zoledronic acid was also reported to downregulate IL-6 gene expression in prostate cancer cells although the underlying mechanism is unclear.[28] In contrast, many therapeutic agents are associated with the upregulation of IL-6 expression, including paclitaxel through the activation of the JNK and Toll-like receptor 4 signaling pathways[29] and the multikinase inhibitor sunitinib through a yet-to-be-identified mechanism.[30] Consequently, understanding the mechanism of this AMPK-independent induction will shed light onto the regulation of IL-6 production.

Recently, two direct, small-molecule activators of AMPK, 4-hydroxy-3-(2′-hydroxy-biphenyl-4-yl)-6-oxo-6,7-dihydro-thieno[2,3-*b*]pyridine-5-carbonitrile (**63**, A-769662) and 5-{5-[5-(2-nitro-4,5-dimethyl-phenyl)-furan-2-ylmethylene]-4-oxo-thiazolidin-2-ylidene-amino}-2-chloro-benzoic acid (**64**, PT1), were discovered, each of which exhibits a unique mode of activation.[16−19] Evidence suggests that allosteric binding of compound **63** to the AMPK γ subunit stabilizes a conformation of AMPK that inhibits dephosphorylation at the Thr-172,[18] while compound **64** antagonizes AMPK autoinhibition by binding to the α subunit near the autoinhibitory domain.[17] Although the mode of protein−ligand recognition remains unclear, molecular docking of compound **64** into AMPK α1 suggests that the binding is mainly attributable to electrostatic interactions.[17] As compound **53** contains many electron-rich moieties as compounds **63** and **64** do, molecular modeling analysis was carried out to compare the electrostatic potential

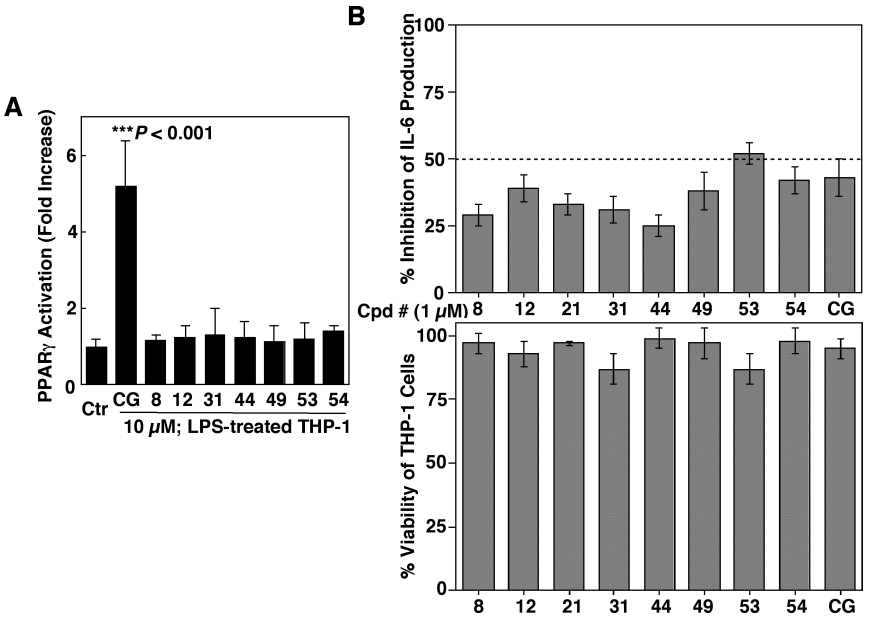

Figure 5. (A) Effects of compounds **8**, **12**, **31**, **44**, **49**, **53**, and **54** vis-à-vis ciglitazone (CG), each at 10 μM, on PPARγ activation in differentiated THP-1 cells. THP-1 cells were transiently transfected with the PPRE-x3-TK-Luc reporter vector and then exposed to individual agents or DMSO vehicle in 10% FBS-supplemented RPMI 1640 medium for 48 h. Analysis of luciferase activity was carried out as described in the Experimental Section. Columns, mean; bars, SD ($N = 6$). (B) Upper panel, ELISA analysis of the inhibitory effects of compounds **8**, **12**, **21**, **31**, **44**, **49**, **53**, and **54** vis-à-vis ciglitazone (CG), each at 1 μM, on LPS-stimulated IL-6 production in THP-1 macrophages in 10% FBS-containing medium after 6 h of treatment. Columns, mean; bars, SD ($N = 3$). Lower panel, the corresponding effects on the viability of THP-1 cells by MTT assays ($N = 6$).

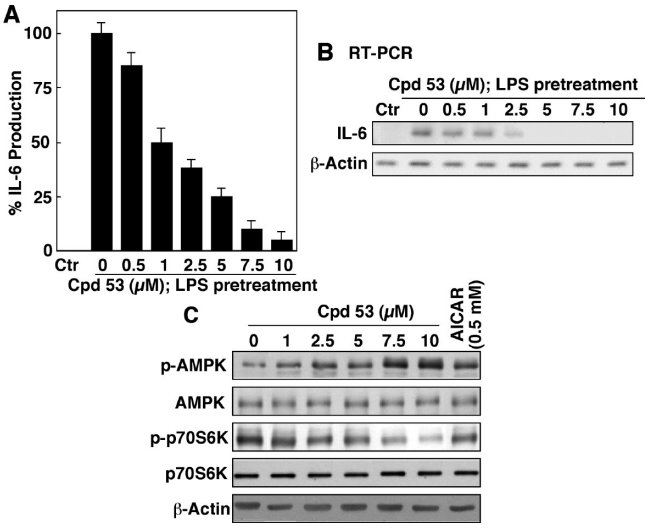

Figure 6. (A) ELISA analysis of the dose-dependent effect of compound **53** on LPS-stimulated IL-6 production in THP-1 macrophages in 10% FBS-containing medium after 6 h of treatment. Columns, mean; bars, SD ($N = 3$). (B) RT-PCR analysis of the dose-dependent suppressive effect of compound **53** on the mRNA levels of IL-6 in LPS-treated THP-1 macrophages in 10% FBS-containing medium after 6 h of treatment. Columns, mean; bars, SD ($N = 3$). (C) Western blot analysis of the dose-dependent effect of compound **53** relative to 0.5 mM AICAR on the phosphorylation levels of AMPK and p70S6K in LPS-treated THP-1 macrophages in 10% FBS-containing medium after 6 h of treatment.

of these compounds (Figure 7D). The electron densities of individual areas are colored in red and blue to indicate positive and negative electrostatic potentials, respectively, and changes in electrostatic potential from positive to negative are seen in transition from red to blue. As shown, the electrostatic potential map of compound **53** exhibited some degree of similarity to that of compound **64**, and, to a lesser extent, compound **63**. This finding suggests that compound **53** might mediate AMPK activation through an allosteric binding mechanism similar to that of compound **63** or **64**, which constitutes the current focus of this investigation.

As AMPK represents a therapeutically relevant target for the treatment of the metabolic syndrome and cancer,[7–9] there is a growing interest in the development of novel pharmacological activators for this fuel-sensing enzyme.[16–19] However, questions remain regarding the potential adverse effects of sustained pharmacological activation of AMPK, especially in the liver and skeletal muscle.[9] In the face of this challenge, understanding the functional role of AMPK isozymes in different tissues as a prelude to designing isozyme-specific activators and/or tissue-selective delivery represents an urgent issue.

Conclusion

In light of the high potency of compound **53** in activating AMPK and inhibiting IL-6 production, it serves as a useful agent to investigate the effects of modulating these two signaling effectors in the therapeutic intervention of different diseases in cell and animal models. In addition, characterization of its mechanism in AMPK activation will shed light onto the functional regulation of AMPK, which might lead to the identification of additional AMPK activators.

Experimental Section

Chemical reagents and organic solvents were purchased from Sigma-Aldrich (St. Louis, MO) unless otherwise mentioned. Nuclear magnetic resonance spectra (^{1}H NMR) were measured on a Bruker DPX 300 model spectrometer. Chemical shifts (δ) were reported in parts per million (ppm) relative to the TMS peak. Electrospray ionization mass spectrometry analyses were performed with a Micromass Q-Tof II high-resolution

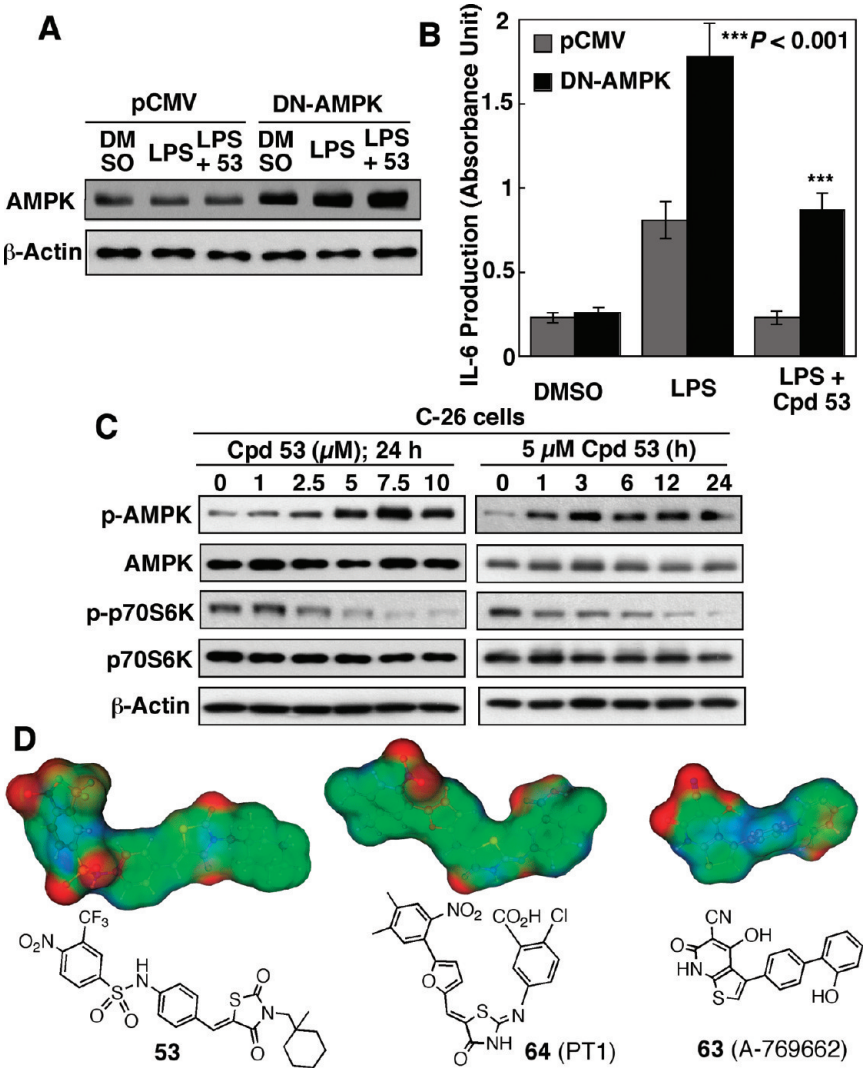

Figure 7. (A) Western blot analysis of the expression levels of AMPK in THP-1 macrophages transiently transfected with the dominant negative (DN)-AMPK plasmid or pCMV empty vector. (B) Protective effect of ectopic expression of DN-AMPK on LPS-stimulated IL-6 production in THP-1 macrophages with or without cotreatment with 10 μM compound **53**. Columns, mean; bars, SD (N = 3). (C) Western blot analysis of the dose- and time-dependent effects of compound **53** on the phosphorylation levels of AMPK and p70S6K in C-26 adenocarcinoma cells in 10% FBS-containing medium. (D) The surface electrostatic potentials and structures of compound **53** versus compounds **63** and **64**.

electrospray mass spectrometer. The purities of all tested compounds are higher than 95% by elemental analyses, which were performed by Atlantic Microlab, Inc. (Norcross, GA), and were reported to be within 0.4% of calculated values. Flash column chromatography was performed using silica gel (230−400 mesh). The structures of the eight lead candidates could be divided into three series, i.e., A (**8**, **12**, and **21**), B (**31** and **44**), and C (**49**, **53**, and **54**) (Figure 1A). The general procedures for the synthesis of series A−C compounds are described in Figure 1B. Compounds of series A and B were synthesized according to slight modifications of previously reported procedures,[20,21] and the synthesis of the series C active compounds (**49**, **53**, and **54**) is illustrated by the synthesis of compound **53** as an example.

5-[3-Bromo-4-(6-ethoxy-2,5,7,8-tetramethyl-chroman-2-ylmethoxy)-benzylide-ne]-thiazolidine-2,4-dione (8). ^{1}H NMR (300 MHz, CDCl3), δ 1.42 (t, J = 7.2 Hz, 3H), 1.51(s, 3H), 1.92−2.03 (m, 1H), 2.05−2.23 (m, 10H), 2.58−2.72 (m, 2H), 3.74 (q, J = 7.2 Hz, 2H), 4.14 (q, J = 9.3 Hz, 2H), 7.00 (d, J = 8.4 Hz, 1H), 7.41 (dd, J = 2.4, 8.4 Hz, 1H), 7. 71 (d, J = 2.4 Hz, 1H), 7.75 (s, 1H), 8.65 (s, 1H). HRMS exact mass of $C_{26}H_{28}BrNO_5S$ $(M + Na)^+$, 568.0769 amu; observed mass of $(M + Na)^+$, 568.0786 amu. Anal. calcd C 57.14, H 5.16, O 14.64; found C 57.23, H 5.26, O 14.66.

5-[4-(6-Butoxy-2,5,7,8-tetramethyl-chroman-2-ylmethoxy)-3-methoxy-benzyli-dene]-thiazolidine-2,4-dione (12). ^{1}H NMR (300 MHz, CDCl3), δ 0.99 (t, J = 7.2 Hz, 3H), 1.45 (s, 3H), 1.52−1.66 (m, 2H), 1.73−1.85 (m, 2H), 1.89−1.99 (m, 1H), 2.02−2.23 (m, 10H), 2.60−2.69 (m, 2H), 3.63 (t, J = 6.6 Hz, 2H), 3.90 (s, 3H), 4.04 (d, J = 9.3 Hz, 1H), 4.12 (d, J = 9.3 Hz, 1H), 6.96−7.10 (m, 3H), 7.80 (s, 1H), 8.58 (br, 1H). HRMS exact mass of $C_{29}H_{35}NO_6S$ $(M + Na)^+$, 548.2083 amu; observed mass of $(M + Na)^+$, 548.2095 amu. Anal. calcd C 66.26, H 6.71, O 18.26; found C 66.32, H 6.80, O 18.29.

4-{2-[2-Bromo-4-(2,4-dioxo-thiazolidin-5-ylidenemethyl)-phenoxymethyl]-2,5,7,8-tetramethyl-chroman-6-yloxy}-butyronitrile (21). ^{1}H NMR (300 MHz, CDCl3), δ 1.49 (s, 3H), 1.94−2.23 (m, 13H), 2.58−2.74 (m, 4H), 3.76 (t, J = 5.7 Hz, 2H), 4.00−4.16 (m, 2H), 6.97 (d, J = 8.7 Hz, 1H), 7.40 (dd, J = 2.1, 8.7 Hz, 1H), 7.70 (d, J = 2.1 Hz, 1H), 7.74 (s, 1H), 8.36 (br, 1H). HRMS exact mass of $C_{28}H_{29}BrN_2O_5S$ $(M + Na)^+$, 607.0878 amu; observed mass of $(M + Na)^+$, 607.0882 amu. Anal. calcd C 57.44, H 4.99, O 13.66; found C 57.54, H 5.04, O 13.72.

5-(4-Hydroxy-3-trifluoromethyl-benzylidene)-3-(1-methyl-cyclohexylmethyl)-thiazolidine-2,4-dione (31). ^{1}H NMR (300 MHz, $CDCl_3$) 0.95 (s, 3H), 1.46−1.56 (m, 10H), 3.64 (s, 2H),

6.08−6.38 (br, 1H), 7.09 (d, J = 8.4 Hz, 1H), 7.59 (d, J = 8.4 Hz, 1H), 7.69 (s, 1H), 7.83 (s, 1H). HRMS exact mass of $C_{19}H_{20}F_3NO_3S$, $(M + Na)^+$, 422.1014 amu; found: 422.1012 amu. Anal. calcd C 57.13, H 5.05, O 12.02; found C 57.38, H 5.04, O 12.16.

5-(4-Hydroxy-3-trifluoromethyl-benzylidene)-3-propyl-thiazolidine-2,4-dione (44). ^{1}H NMR (300 MHz, $CDCl_3$) 0.97 (t, J = 7.5 Hz, 3H), 1.60−1.78 (m, 2H), 3.74 (t, J = 7.5 Hz, 2H), 6.19 (br, 1H), 7.09 (d, J = 8.4 Hz, 1H), 7.59 (d, J = 8.4 Hz, 1H), 7.69 (s, 1H), 7.83 (s, 1H). HRMS exact mass of $C_{14}H_{12}F_3NO_3S$, $(M + Na)^+$, 331.3112 amu; found: 331.3124 amu. Anal. calcd C 50.75, H 3.65, O 14.49; found C 50.84, H 3.68, O 14.54.

***N*-{4-[3-(1-Methyl-cyclohexylmethyl)-2,4-dioxo-thiazolidin-5-ylidene-methyl]-phenyl}-4-nitro-3-trifluoromethyl-benzenesulfonamide (53). Step a.** Trifluoro-methanesulfonic acid 1-methyl-cyclohexylmethyl ester (i) was prepared from 1-methyl-cyclohexanecarboxylic acid as previously described.[21] A mixture of i (0.5 mmol), 2,4-thiazolidinedione (0.6 mmol) and K_2CO_3 (0.7 mmol) were dissolved in DMF (3 mL), heated to 80 °C with stirring for 4 h, poured into water, extracted with ethyl acetate (10 mL) three times, and concentrated. The residue was purified by flash column chromatography to afford 3-(1-methyl-cyclohexylmethyl)-thiazolidine-2,4-dione (ii) in 50% yield.

Step b. To a mixture of methyl 4-aminobenzoate (1.51 g, 10 mmol) and pyridine (0.97 mL) in dry methylene chloride (100 mL), 4-nitro-3-trifluoromethylbenzenesulfonyl chloride (2.89 g, 10 nmol) in dry methylene chloride (20 mL) was added slowly and washed, in tandem, with 1N HCl, water, 10% Na_2CO_3 aqueous solution, and brine. The organic layer was dried, filtered, and concentrated. The residue was purified by chromatography (EtOAc-hexane, 1:5) to give 4-(4-nitro-3-trifluoromethyl-phenyl-sulfamoyl)-benzoic acid methyl ester (iii) as colorless crystal with 86% yield. ^{1}H NMR (300 MHz, $CDCl_3$) δ 3.79 (s, 3H), 7.25 (d, J = 5.58 Hz, 2H), 7.85 (d, J = 6.72 Hz, 2H), 7.94 (d, J = 8.43 Hz, 1H), 8.16 (d, J = 8.64 Hz, 1H), 8.30 (s, 1H).

Step c. To a solution of compound iii (3.26 g, 8.06 mmol) in dry THF (50 mL), LAH pallet (0.46 g, 12.10 mmol) was added at 0 °C. The resulting reaction mixture was stirred for 4 h, quenched by the addition of water (5 mL), concentrated, diluted with ethyl acetate (50 mL), and washed, in tandem, with 1N HCl, water, 10% Na_2CO_3 aqueous solution, and brine. The organic layer was dried, filtered, and concentrated. The residue was purified by silica gel chromatography (ethyl acetate−hexane, 3:7) to afford 4-hydroxymethyl-*N*-(4-nitro-3-trifluoromethyl-phenyl)-benzenesulfonamide (iv) as light-yellow solid with 71% yield. ^{1}H NMR (300 MHz, CDCl3) δ 2.06 (br, 1H), 4.75 (s, 2H), 6.96 (br, 1H), 7.59 (d, J = 10.17 Hz, 2H), 7.84 (d, J = 8.19 Hz, 2H), 7.88 (d, J = 8.43 Hz, 1H), 8.03 (d, J = 8.43 Hz, 1H), 8.16 (s, 1H).

Step d. A reaction mixture of compound iv (2.00 g, 5.31 mmol) and MnO_2 (2.34 g, 26.57 mmol) in chloroform (100 mL) was refluxed overnight, concentrated, diluted with ethyl acetate, filtered, and concentrated. The residue was purified by silica gel chromatography (ethyl acetate−hexane, 1:7) to yield *N*-(4-formyl-phenyl)-4-nitro-3-trifluoromethyl-benzenesulfonamide (v) as light-yellow solid in 88% yield. ^{1}H NMR (300 MHz, $CDCl_3$) δ 7.28 (d, J = 6.76 Hz, 2H), 7.88 (d, J = 6.72 Hz, 2H), 7.97 (d, J = 8.43 Hz, 1H), 8.17 (d, J = 8.64 Hz, 1H), 8.31 (s, 1H).

Step e. A reaction mixture of compound ii (0.73 g, 3.21 mmol), compound vi (1.25 g, 3.21 mmol), and catalytic amount of piperidine in ethyl alcohol (50 mL) was refluxed overnight, concentrated, dissolved in ethyl acetate (50 mL), neutralized with acetic acid, washed with water and brine, dried, and concentrated. The residue was purified by silica gel chromatography (ethyl acetate−hexane, 1:7) to give afforded compound **53** as yellow solid in 72% yield. ^{1}H NMR (300 MHz, DMSO-*d*) δ 0.80 (s, 3H), 1.20−1.43 (m, 10H), 3.47 (s, 2H), 7.24 (d, J = 7.65 Hz. 2H), 7.52 (d, J = 8.28 Hz, 2H), 7.78 (s, 1H), 8.26 (s, 1H), 8.31 (s, 1H), 11.12 (br, 1H). HRMS exact mass of $C_{25}H_{24}F_3N_3O_6S_2$, $(M + Na)^+$, 606.0956 amu; found: 606.0974 amu. Anal. calcd C 51.45, H 4.15, O 16.45; found C 51.72, H 4.20, O 16.54.

4-Methoxy-*N*-{4-[3-(1-methyl-cyclohexylmethyl)-2,4-dioxo-thiazolidin-5-yli-denemethyl]-phenyl}-benzenesulfonamide (49). ^{1}H NMR (300 MHz, CDCl3/MeOD-d_4) 0.96 (s, 3H), 1.22−1.62 (m, 10H), 3.66 (s, 2H), 3.91 (s, 3H), 7.02 (d, J = 8.7 Hz, 2H), 7.55 (d, J = 8.7 Hz, 2H), 7.79 (d, J = 8.1 Hz, 2H), 7.87(d, J = 8.1 Hz, 2H), 7.88 (s, 1H). HRMS exact mass of $C_{26}H_{28}N_2O_5S_2$, $(M + Na)^+$, 535.1337 amu; found: 535.1352 amu. Anal. calcd C 60.92, H 5.51, O 15.60; found C 60.72, H 5.60, O 15.54.

***N*-{4-[3-(1-Methyl-cyclohexylmethyl)-2,4-dioxo-thiazolidin-5-ylidenemethyl]-phenyl}-4-nitro-benzenesulfonamide (54).** ^{1}H NMR (300 MHz, *d*-DMSO), δ 0.82 (s, 3H), 1.21−1.45 (m, 10H), 3.51 (s, 2H), 7.24 (d, J = 8.55 Hz, 2H), 7.51(d, J = 8.55 Hz, 2H), 7.78 (s, 1H), 8.04 (d, J = 9.00 Hz, 2H), 8.36 (d, J = 8.97 Hz, 2H), 11.12 (br, 1H). HRMS exact mass of $C_{24}H_{25}N_3O_6S_2$, $(M + Na)^+$, 538.1083 amu; found: 538.1092 amu. Anal. calcd C 55.91, H 4.89, O 18.62; found C 55.98, H 4.98, O 18.76.

Cells and Cell Culture. THP-1 monocytic cells were purchased from the American Type Culture Collection (Rockville, MD) and maintained with L-glutamine-containing RPMI 1640 supplemented with 10% fetal bovine serum (FBS), 0.25% glucose, 0.01% sodium pyruvate, 50 μM 2-mercaptoethanol, and 0.1 mL/mL penicillin/streptomycin/L-glutamine. Differentiation of THP-1 monocytes into macrophages was carried out by exposure to PMA (50 nM) in the aforementioned RPMI 1640 medium for 24 h. Colon-26 (C-26) adenocarcinoma cells were a kind gift of Dr. Denis Guttridge (The Ohio State University). The C-26 cells were maintained in RPMI 1640 medium supplemented with 5% FBS and 1% penicillin/streptomycin. All cell types were cultured at 37 °C in a humidified incubator containing 5% CO_2.

Cell Viability Assay. Cell viability was determined using the 3-(4,5-dimethylthiazol-2-yl)-2,5-diphenyltetrazolium bromide) (MTT) assay. Cells were seeded in 96-well plates (5000 cells/well) and incubated in 10% FBS-supplemented medium for 24 h and were then treated with individual agents for 72 h. Drug-containing medium was then replaced with MTT (0.5 mg/mL in RPMI 1640), followed by incubation at 37 °C for 2 h. After removal of medium, the reduced MTT dye was solubilized in 200 μL/well DMSO, and absorbance at 570 nm was measured.

ELISA. IL-6 release by differentiated THP-1 macrophages in response to 10 ng/mL of LPS was analyzed by using the IL-6 ELISA kit (Cayman Chemical Co., Ann Arbor, MI) according to the manufacturer's instruction in triplicate. The effect of each test compound on LPS-stimulated IL-6 release is presented as percent inhibition and was calculated using the following formula: percentage inhibition = 100% × {1 − [(O.D. of sample − O.D. of control)/(O.D. of LPS − O.D. of control)]}.

Western Blotting. THP-1 cells were lysed in SDS-sample buffer after washing with iced-PBS buffer and then heated at 95 °C for 20 min. Protein extracts were prepared using M-PER mammalian protein extraction reagent (Pierce, Rockford, IL) containing freshly added 1% phosphatase and protease inhibitor cocktails (Calbiochem). After centrifugation of lysates at 13000*g* for 10 min, supernatants were collected and the protein concentration in each sample was determined by protein assay (Bio-Rad). Protein extracts were then suspended in 2× SDS sample buffer, separated by electrophoresis in 10% SDS-polyacrylamide gels, and transferred to nitrocellulose membranes using a semidry transfer cell. The transblotted membrane was washed twice with Tris-buffered saline containing 0.1% Tween-20 (TBST). After blocking with TBST containing 5% nonfat milk for 1 h, the membrane was incubated with primary antibodies: p^{172}Thr-AMPK, AMPK, p^{705}Tyr-Stat3 and Stat3 (Cell Signaling Technology; Beverly, MA), p^{389}Thr-p70S6K and p70S6K (Santa Cruz Biotechnology; Santa Cruz, CA), each at 1:1000 dilution in 1% TBST-nonfat milk at 4 °C overnight. After incubation with the primary antibody, the membrane was

washed three times with TBST for a total of 30 min, followed by incubation with horseradish peroxidase-conjugated goat anti-mouse IgG (diluted 1:2500) for 1 h at room temperature. After three thorough washes with TBST for a total of 30 min, the immunoblots were visualized by enhanced chemiluminescence.

Transient Transfection. Transfection of THP-1 cells with the K45R kinase-dead, dominant-negative AMPK plasmid (Addgene, Cambridge, MA) or empty vector was performed by electroporation using the Human Monocyte Nucleofector Kit of the Amaxa Nucleofector System (Amaxa Biosystems, Cologne, Germany) according to a published procedure.[31]

Analysis of PPARγ Activation. The PPRE-x3-TK-Luc reporter vector containing three copies of the PPAR response elements preceding the thymidine kinase promoter-luciferase construct was used for detection of PPARγ activation.[32] Differentiated THP-1 macrophages were plated at the density of 1×10^5 cells/per well in 24-well plates and then transiently transfected by nucleofection with the PPRE-x3-TK-Luc reporter plasmid followed by exposure to 10 μM ciglitazone or its derivatives in triplicate in the presence of LPS for 48 h. Cells were lysed with passive lysis buffer (Promega), and aliquots of the lysates (50 μL) were transferred to 96-well plates and mixed with 100 μL of luciferase substrate (Promega). Luciferase activity was determined by using the MicroLumatPlus LB96 V luminometer (Berthold Technologies, Oak Ridge, TN) with the WinGlow software package.

Total RNA Isolation and RT-PCR Analysis of IL-6 Expression. Total RNA was extracted from drug- or vehicle-treated THP-1 macrophages with TRIzol (Invitrogen, Carlsbad, CA) and then reverse-transcribed to cDNA using the Omniscript RT Kit (Qiagen, Valencia, CA). The sequences of the primers used for RT-PCR were as follows:

IL-6: forward, 5′-GAGAAAGGAGACATGTAACAAGAGT-3′, reverse 5′-GCGCAGA-ATGAGATGAGTTGT-3′; β-actin: forward, 5′-TCTACAATGAGCTGCGTGTG-3′, reverse, 5′-GGTCAGGATCTTCATGAGGT-3′. The PCR products were separated by electrophoresis on 1% agarose gels and visualized by ethidium bromide staining.

Molecular Model Experiment. Molecular structures of compound **53**, **63**, and **64** were initially subjected to 1000 steps of Monte Carlo simulation using Merck Molecular Force Field program available in Spartan 08 (Wavefuction, Inc., Irvine, Ca; http://www.wavefun.com/). The minimum conformation reached by the simulation was then fully optimized at a density function theory level of B3LYP/6-31G* with Gaussian 03 (Gaussian, Inc., Wallingford, CT; http://www.gaussian.com/). All the fully optimized structures were confirmed by normal-mode analysis; no negative frequencies were found. Computations for electrostatic potential and density were carried out for each optimal structure by potential population analysis under Hartree−Fock/6-31G* function theory by using Gaussian 03. The electrostatic potential map for each compound was generated by Molecular Operation Environment 2008.10 (Chemical Computing Group, Montreal, Canada; http://www.chemcomp.com/) and are presented with the electrostatic potential mapped onto the electron density.

Acknowledgment. This work is supported by National Institutes of Health Grant CA112250 and the Lucius A. Wing Endowed Chair Fund at The Ohio State University.

References

(1) Kahn, B. B.; Alquier, T.; Carling, D.; Hardie, D. G. AMP-activated protein kinase: ancient energy gauge provides clues to modern understanding of metabolism. *Cell Metab*. **2005**, *1*, 15–25.
(2) Hardie, D. G.; Sakamoto, K. AMPK: a key sensor of fuel and energy status in skeletal muscle. *Physiology* **2006**, *21*, 48–60.
(3) Hardie, D. G. AMP-activated/SNF1 protein kinases: conserved guardians of cellular energy. *Nat. Rev. Mol. Cell Biol*. **2007**, *8*, 774–785.
(4) Inoki, K.; Zhu, T.; Guan, K. L. TSC2 mediates cellular energy response to control cell growth and survival. *Cell* **2003**, *115*, 577–590.
(5) Lihn, A. S.; Pedersen, S. B.; Lund, S.; Richelsen, B. The anti-diabetic AMPK activator AICAR reduces IL-6 and IL-8 in human adipose tissue and skeletal muscle cells. *Mol. Cell. Endocrinol*. **2008**, *292*, 36–41.
(6) Sag, D.; Carling, D.; Stout, R. D.; Suttles, J. Adenosine 5′-monophosphate-activated protein kinase promotes macrophage polarization to an anti-inflammatory functional phenotype. *J. Immunol*. **2008**, *181*, 8633–8641.
(7) Carling, D. The AMP-activated protein kinase cascade—a unifying system for energy control. *Trends Biochem. Sci*. **2004**, *29*, 18–24.
(8) Luo, Z.; Saha, A. K.; Xiang, X.; Ruderman, N. B. AMPK, the metabolic syndrome and cancer. *Trends Pharmacol. Sci*. **2005**, *26*, 69–76.
(9) Zhang, B. B.; Zhou, G.; Li, C. AMPK: an emerging drug target for diabetes and the metabolic syndrome. *Cell Metab*. **2009**, *9*, 407–416.
(10) Viollet, B.; Mounier, R.; Leclerc, J.; Yazigi, A.; Foretz, M.; Andreelli, F. Targeting AMP-activated protein kinase as a novel therapeutic approach for the treatment of metabolic disorders. *Diabetes Metab*. **2007**, *33*, 395–402.
(11) Rattan, R.; Giri, S.; Singh, A. K.; Singh, I. 5-Aminoimidazole-4-carboxamide-1-beta-D-ribofuranoside inhibits cancer cell proliferation in vitro and in vivo via AMP-activated protein kinase. *J. Biol. Chem*. **2005**, *280*, 39582–39593.
(12) Fryer, L. G.; Parbu-Patel, A.; Carling, D. The Anti-diabetic drugs rosiglitazone and metformin stimulate AMP-activated protein kinase through distinct signaling pathways. *J. Biol. Chem*. **2002**, *277*, 25226–25232.
(13) Konrad, D.; Rudich, A.; Bilan, P. J.; Patel, N.; Richardson, C.; Witters, L. A.; Klip, A. Troglitazone causes acute mitochondrial membrane depolarisation and an AMPK-mediated increase in glucose phosphorylation in muscle cells. *Diabetologia* **2005**, *48*, 954–966.
(14) Corton, J. M.; Gillespie, J. G.; Hawley, S. A.; Hardie, D. G. 5-Aaminoimidazole-4-carboxamide ribonucleoside. A specific method for activating AMP-activated protein kinase in intact cells? *Eur. J. Biochem*. **1995**, *229*, 558–565.
(15) Towler, M. C.; Hardie, D. G. AMP-activated protein kinase in metabolic control and insulin signaling. *Circ. Res*. **2007**, *100*, 328–341.
(16) Cool, B.; Zinker, B.; Chiou, W.; Kifle, L.; Cao, N.; Perham, M.; Dickinson, R.; Adler, A.; Gagne, G.; Iyengar, R.; Zhao, G.; Marsh, K.; Kym, P.; Jung, P.; Camp, H. S.; Frevert, E. Identification and characterization of a small molecule AMPK activator that treats key components of type 2 diabetes and the metabolic syndrome. *Cell Metab*. **2006**, *3*, 403–416.
(17) Pang, T.; Zhang, Z. S.; Gu, M.; Qiu, B. Y.; Yu, L. F.; Cao, P. R.; Shao, W.; Su, M. B.; Li, J. Y.; Nan, F. J.; Li, J. Small molecule antagonizes autoinhibition and activates AMP-activated protein kinase in cells. *J. Biol. Chem*. **2008**, *283*, 16051–16060.
(18) Sanders, M. J.; Ali, Z. S.; Hegarty, B. D.; Heath, R.; Snowden, M. A.; Carling, D. Defining the mechanism of activation of AMP-activated protein kinase by the small molecule A-769662, a member of the thienopyridone family. *J. Biol. Chem*. **2007**, *282*, 32539–32548.
(19) Zhao, G.; Iyengar, R. R.; Judd, A. S.; Cool, B.; Chiou, W.; Kifle, L.; Frevert, E.; Sham, H.; Kym, P. R. Discovery and SAR development of thienopyridones: a class of small molecule AMPK activators. *Bioorg. Med. Chem. Lett*. **2007**, *17*, 3254–3257.
(20) Huang, J. W.; Shiau, C. W.; Yang, J.; Wang, D. S.; Chiu, H. C.; Chen, C. Y.; Chen, C. S. Development of small-molecule cyclin D1-ablative agents. *J. Med. Chem*. **2006**, *49*, 4684–4689.
(21) Yang, J.; Wei, S.; Wang, D. S.; Wang, Y. C.; Kulp, S. K.; Chen, C. S. Pharmacological exploitation of the peroxisome proliferator-activated receptor gamma agonist ciglitazone to develop a novel class of androgen receptor-ablative agents. *J. Med. Chem*. **2008**, *51*, 2100–2107.
(22) Auwerx, J. The human leukemia cell line, THP-1: a multifacetted model for the study of monocyte-macrophage differentiation. *Experientia* **1991**, *47*, 22–31.
(23) Wang, L.; Damania, B. Kaposi's sarcoma-associated herpesvirus confers a survival advantage to endothelial cells. *Cancer Res*. **2008**, *68*, 4640–4648.
(24) Fujimoto-Ouchi, K.; Tamura, S.; Mori, K.; Tanaka, Y.; Ishitsuka, H. Establishment and characterization of cachexia-inducing and -non-inducing clones of murine colon 26 carcinoma. *Int. J. Cancer* **1995**, *61*, 522–528.
(25) Guo, D.; Hildebrandt, I. J.; Prins, R. M.; Soto, H.; Mazzotta, M. M.; Dang, J.; Czernin, J.; Shyy, J. Y.; Watson, A. D.; Phelps, M.; Radu, C. G.; Cloughesy, T. F.; Mischel, P. S. The AMPK agonist AICAR inhibits the growth of EGFRvIII-expressing glioblastomas by

inhibiting lipogenesis. *Proc. Natl. Acad. Sci. U.S.A* **2009**, *106*, 12932–12937.
(26) Jang, S.; Kelley, K. W.; Johnson, R. W. Luteolin reduces IL-6 production in microglia by inhibiting JNK phosphorylation and activation of AP-1. *Proc. Natl. Acad. Sci. U.S.A* **2008**, *105*, 7534–7539.
(27) Jang, C. H.; Choi, J. H.; Byun, M. S.; Jue, D. M. Chloroquine inhibits production of TNF-alpha, IL-1beta and IL-6 from lipopolysaccharide-stimulated human monocytes/macrophages by different modes. *Rheumatology* (*Oxford, U.K.*) **2006**, *45*, 703–710.
(28) Asbagh, L. A.; Uzunoglu, S.; Cal, C. Zoledronic acid effects interleukin-6 expression in hormone-independent prostate cancer cell lines. *Int. Braz. J. Urol.* **2008**, *34*, 355−363; discussion 364.
(29) Wang, T. H.; Chan, Y. H.; Chen, C. W.; Kung, W. H.; Lee, Y. S.; Wang, S. T.; Chang, T. C.; Wang, H. S. Paclitaxel (Taxol) upregulates expression of functional interleukin-6 in human ovarian cancer cells through multiple signaling pathways. *Oncogene* **2006**, *25*, 4857–4866.
(30) Nishioka, C.; Ikezoe, T.; Yang, J.; Yokoyama, A. Multitargeted tyrosine kinase inhibitor stimulates expression of IL-6 and activates JAK2/STAT5 signaling in acute myelogenous leukemia cells. *Leukemia* **2009**, *23*, 2304–2308.
(31) Schnoor, M.; Buers, I.; Sietmann, A.; Brodde, M. F.; Hofnagel, O.; Robenek, H.; Lorkowski, S. Efficient nonviral transfection of THP-1 cells. *J. Immunol. Methods* **2009**, *344*, 109–115.
(32) Yang, C. C.; Wang, Y. C.; Wei, S.; Lin, L. F.; Chen, C. S.; Lee, C. C.; Lin, C. C. Peroxisome proliferator-activated receptor gamma-independent suppression of androgen receptor expression by troglitazone mechanism and pharmacologic exploitation. *Cancer Res.* **2007**, *67*, 3229–3238.